https://doi.org/10.5194/acp-2022-6
Preprint. Discussion started: 27 January 2022


Atmospheric Chemistry and Physics Discussions

# The Positive Effect of Formaldehyde on the Photocatalytic Renoxification of Nitrate on $TiO_2$ Particles

Yuhan Liu, Xuejiao Wang, Mengshuang Sheng, Chunxiang Ye, Jing Shang*

*State Key Joint Laboratory of Environmental Simulation and Pollution Control, College of Environmental Sciences and Engineering, Peking University, 5 Yiheyuan Road, Beijing 100871, P. R. China*

Corresponding author: Jing Shang

Email: shangjing@pku.edu.cn

**Abstract**

Renoxification is the recycling of $NO_3^-$/$HNO_3$ into $NO_x$ under illumination; it is promoted by the photocatalysis of $TiO_2$. Formaldehyde (HCHO), the most abundant carbonyl compound in the atmosphere, may participate in the renoxification of nitrate-doped $TiO_2$ ($NO_3^-$-$TiO_2$) aerosols. In this study, we established an environmental chamber reaction system under different light sources, excluding direct photolysis of nitrate by adjusting the illumination wavelength, to explore the photocatalytic renoxification process. It is suggested that HCHO and $TiO_2$ have a significant synergistic effect on photocatalytic renoxification via the $NO_3^-$-$NO_3$·-HCHO-$HNO_3$-$NO_x$ pathway. Adsorbed HCHO may react with nitrate radicals through hydrogen abstraction to form $HNO_3$ on the surface, resulting in the

https://doi.org/10.5194/acp-2022-6
Preprint. Discussion started: 27 January 2022


Atmospheric Chemistry and Physics Discussions

mass generation of $NO_x$. We found that for 4 wt% $NO_3^-$-$TiO_2$ aerosols (e.g., $KNO_3$-$TiO_2$), the $NO_x$ concentration reached up to 110 ppb, and was 2 orders of magnitude higher than in the absence of HCHO. Nitrate type and contents, relative humidity, and HCHO concentration were found to influence $NO_x$ release. The significant synergistic enhancement effect of renoxification affects photochemical processes such as atmospheric oxidation and nitrogen cycling on the surfaces of particles containing semiconductor oxides, with the participation of hydrogen donor organics.

## 1 Introduction

The levels of ozone ($O_3$) and hydroxyl radicals (·OH) in the troposphere can be promoted by nitrogen oxides ($NO_x$ = NO + $NO_2$), such that $NO_x$ plays an important role in the formation of secondary aerosols and atmospheric oxidants (Platt et al., 1980; Stemmler et al., 2006; Harris et al., 1982; Finlayson-Pitts and Pitts, 1999). $NO_x$ can be converted into nitric acid ($HNO_3$) and nitrate ($NO_3^-$) through a series of oxidation and hydrolysis reactions and is eventually removed from the atmosphere through subsequent wet or dry deposition (Dentener and Crutzen, 1993; Goodman et al., 2001; Monge et al., 2010; Bedjanian and El Zein, 2012). However, comparisons of observations and modeling results for the marine boundary layer, land, and free troposphere (Read et al., 2008; Lee et al., 2009; Seltzer et al., 2015) have shown underestimation of $HNO_3$ or $NO_3^-$ content, $NO_x$ abundance, and $NO_x$/$HNO_3$ ratios, indicating the presence of a new, rapid $NO_x$ circulation pathway (Ye et al., 2016b;

https://doi.org/10.5194/acp-2022-6
Preprint. Discussion started: 27 January 2022


Atmospheric Chemistry and Physics Discussions

Reed et al., 2017). Some researchers have suggested that deposited $NO_3^-$ and $HNO_3$ can be recycled back to gas phase $NO_x$ under illumination, via the renoxification process (Schuttlefield et al., 2008; Romer et al., 2018; Bao et al., 2020; Shi et al., 2021b). Photolytic renoxification occurs under light with a wavelength of < 350 nm, through the photolysis of $NO_3^-$/$HNO_3$ adsorbed on the solid surface to generate $NO_x$. Notably, the photolysis of $NO_3^-HNO_3$ is reported to occur at least 2 orders of magnitude faster on different solid surfaces (natural or artificial) or aerosols than in the gas phase (Ye et al., 2016a; Zhou et al., 2003; Baergen and Donaldson, 2013). Several recent studies have shown that renoxification has important atmospheric significance (Deng et al., 2010; Kasibhatla et al., 2018; Romer et al., 2018; Alexander et al., 2020), providing the atmosphere with a new source of photochemically reactive nitrogen species, i.e., HONO or $NO_x$, resulting in the production of more photooxidants such as $O_3$ or ·OH (Ye et al., 2017), which further oxidize volatile organic compounds (VOCs), leading to the formation of more chromophores, thereby affecting the photochemical process (Bao et al., 2020).

Renoxification processes have recently been observed on different types of atmospheric particles, such as urban grime and mineral dust (Ninneman et al., 2020; Bao et al., 2018; Baergen and Donaldson, 2013; Ndour et al., 2009). Atmospheric titanium dioxide ($TiO_2$) is mainly derived from windblown mineral dust, with mass mixing ratios ranging from 0.1 to 10% (Chen et al., 2012). $TiO_2$ is widely used in industrial processes and building exteriors for its favorable physical and chemical properties. Titanium and nitrate ions have been found to coexist in atmospheric

https://doi.org/10.5194/acp-2022-6
Preprint. Discussion started: 27 January 2022


Atmospheric Chemistry and Physics Discussions

67 particulates in different regions worldwide (Sun et al., 2005; Schwartz-Narbonne et al.,
68 2019). The relative content of $TiO_2$ and $NO_3^-$ in atmospheric particles varies greatly,
69 and nitrate-coated $TiO_2$ ($NO_3^-$-$TiO_2$) aerosols containing $TiO_2$ as the main body can
70 be used to effectively represent particles for sandstorm modeling (Sun et al., 2005;
71 Kim et al., 2012). $TiO_2$ is a semiconductor metal oxide that can facilitate the
72 photolysis of nitrate and the release of $NO_x$ due to its photocatalytic activity (Ndour et
73 al., 2009; Chen et al., 2012; Verbruggen, 2015; Schwartz-Narbonne et al., 2019).
74 Under ultraviolet (UV) light, $TiO_2$ generates electron-hole pairs in the conduction and
75 valence bands, respectively (Linsebigler et al., 1995). Nitrate ions adsorbed at the
76 oxide surface react with the photogenerated holes ($h^+$) to form nitrate radicals ($NO_3\cdot$),
77 which are subsequently photolyzed to $NO_x$, mainly under visible light illumination
78 (Schuttlefield et al., 2008; George et al., 2015; Schwartz-Narbonne et al., 2019). Thus,
79 the renoxification of $NO_3^-$ is faster on $TiO_2$ than on other oxides in mineral dust
80 aerosols such as $SiO_2$ or $Al_2O_3$ (Lesko et al., 2015; Ma et al., 2021). In this study, we
81 refer to renoxification involving $h^+$ and $NO_3^-$ in the reaction as photocatalytic
82 renoxification based on the photocatalytic properties of $TiO_2$.

83 Many previous studies have focused mainly on particulate nitrate-$NO_x$
84 photochemical cycling reactions, despite the potential impact of other reactant gases
85 in the atmosphere. Formaldehyde (HCHO), the most abundant carbonyl compound in
86 the atmosphere, which can react at night with $NO_3\cdot$ via hydrogen abstraction reactions
87 to form $HNO_3$ (Atkinson, 1991). Our previous study showed that the degradation rate
88 of HCHO was faster on $NO_3^-$-$TiO_2$ aerosols than on $TiO_2$ particles, perhaps as a result

https://doi.org/10.5194/acp-2022-6
Preprint. Discussion started: 27 January 2022


Atmospheric Chemistry and Physics Discussions

of HCHO oxidation by $NO_3$·(Shang et al., 2017). To date, no studies have reported the effect of HCHO on photocatalytic renoxification. Adsorbed HCHO would react with $NO_3$· generated on the $NO_3^-$-$TiO_2$ aerosol surface, thus alter the surface nitrogenous species and renoxification process. The present study is the first to explore the combined effect of HCHO and photocatalytic $TiO_2$ particles on the renoxification of nitrate. The wavelengths of the light sources were adjusted to exclude photolytic renoxification while making photocatalytic renoxification available for better elucidate the reaction mechanism. We investigated the effects of various influential factors including nitrate type, nitrate content, RH, and initial HCHO concentration, to understand the atmospheric renoxification of nitrate in greater detail.

## 2 Methods

### 2.1 Environmental chamber setup

Details of the experimental apparatus and protocol used in the current study have been previously described (Shang et al., 2017). Briefly, the main body of the environmental chamber is a 400 L polyvinyl fluoride (PVF) bag filled with synthetic air (high purity $N_2$ (99.999%) mixed with high purity $O_2$ (99.999%) in the ratio of 79:21 by volume, Beijing Huatong Jingke Gas Chemical Co.). The chamber is capable of temperature (~293 K) and relative humidity (0.8–70%) control using a water bubbler and air conditioners, respectively. The chamber is equipped with two light sources both with the central wavelength of 365 nm. One is a set of tube lamps with a main spectrum of 320–400 nm and a small amount of 480-600 nm visible light (Figure S1a). The other is a set of Light-emitting diode (LED) lamps with a narrow main spectrum of 350-390

https://doi.org/10.5194/acp-2022-6
Preprint. Discussion started: 27 January 2022


Atmospheric Chemistry and Physics Discussions

nm (Figure S1b). The light intensities for the tube and LED lamp at 365 nm were 300 $\mu W \cdot cm^{-2}$ and 200 $\mu W \cdot cm^{-2}$, respectively, measured in the middle of the chamber. Aerosol samples were introduced into the chamber by a transient high-pressure airflow. $NO_x$ concentrations at the outlet of the chamber were monitored by a chemiluminescence $NO_x$ analyzer (ECOTECH, EC9841B). HCHO was generated by thermolysis of paraformaldehyde at 70 °C and detected via acetyl acetone spectrophotometric method using a UV-Vis spectrophotometer (PERSEE, T6) or a fluorescence spectrophotometer (THERMO, Lumina), depending on different initial HCHO concentrations. The particle size distribution was measured by a Scanning Nano Particle Spectrometer (HCT, SNPS-20). Electron Spin Resonance (Nuohai Life Science, MiniScope MS 5000) was used to measure ·OH on the surface of particles. 5,5-dimethl-1-pyrroline-N-oxide (DPMO, Enzo) was used as the capture agent. 50 μL particle-containing suspension mixed with 50 μL DMPO (concentration of 200 μM) was loaded in a 1 mm capillary. Four 365 nm LED lamps were placed side by side vertically at a distance of about 1 cm from the capillary, and the measurement was carried out after 1 min of irradiation. The modulation frequency was 100 kHz, the modulation amplitude was 0.2 mT, the microwave power was 10 mW and the sweep time was 60 s.

### 2.2 Nitrate-$TiO_2$ composite samples

In our experiments, two nitrate salts, potassium nitrate (AR, Beijing Chemical Works Co., Ltd) or ammonium nitrate (AR, Beijing Chemical Works Co., Ltd), were complexed with pure $TiO_2$ (≥ 99.5%, Degussa AG) powder or $TiO_2$ (1 wt.%)/$SiO_2$

https://doi.org/10.5194/acp-2022-6
Preprint. Discussion started: 27 January 2022


Atmospheric Chemistry and Physics Discussions

mixed powder to prepare $NO_3^-$-$TiO_2$ or $NO_3^-$-$TiO_2$ (1 wt.%)/$SiO_2$ samples. $TiO_2$ was simply mixed in nitrate solutions at the desired mass mixing ratio (with nitrate content of 1 wt.%, 4 wt.%, 20 wt.%, 80 wt.% and 95 wt.%) to obtain a mash. The mash was dried at 90 °C and then ground carefully to ensure a uniform composite of particles. $SiO_2$ (AR, Xilong Scientific Co., Ltd.) with no optical activity was also chosen for comparison, and samples of $KNO_3$-$SiO_2$ and $KNO_3$-$TiO_2$(1 wt.%)/$SiO_2$ samples with a potassium nitrate content of 4 wt.% were prepared. The blank $TiO_2$ sample was solved in pure water with the same procedure as mentioned above. 4 wt.% $HNO_3$-$TiO_2$ composite particles were prepared for comparison. Concentrated nitric acid (AR, Beijing Chemical Works Co., Ltd) was diluted to 1 M and $TiO_2$ was added to the nitric acid solution and stirred evenly. A layer of aluminum foil was covered on the surface of the $HNO_3$-$TiO_2$ homogenate and dried naturally in the room. After air-drying, follow the same steps above to grind for use. We also selected Arizona Test Dust (ATD, Powder Technology Inc.), whose chemical composition and weight percentage were shown in Table S1, as a substitute of $NO_3^-$/$TiO_2$ to investigate the "photocatalytic renoxification" process of nitrate and the positive effect of HCHO.

**2.3 Environmental chamber experiments**

The experiments carried out in the environmental chamber can be divided into two categories according to whether HCHO was involved or not. (1) No HCHO involvement in the reaction. The PVF bag was inflated by 260 L synthetic air, and then 75 mg $TiO_2$ particles were sprayed into PVF bag. As shown in Figure S2, the concentration of the particles decreased rapidly due to the sedimentation of the larger

https://doi.org/10.5194/acp-2022-6
Preprint. Discussion started: 27 January 2022


Atmospheric Chemistry and Physics Discussions

particles and the electrostatic adsorption of the particles by the environmental chamber. The size distribution of $TiO_2$ reached stable after about 60 min with the peak particle size was about 120 nm, similar to that of atmospheric particles in some urban areas in China (Wang et al., 2015; Li et al., 2019). The size distribution could maintain for more than 4 hours, with the number concentration in the chamber decreased by no more than 5% per hour. (2) With the participation of HCHO. The PVF bag was inflated by 125 L synthetic air, followed by the introduction of HCHO, and then the chamber was filled up with zero air to about 250 L. It can be seen from Figure S3 that it took about 60 min for the HCHO concentration to reach stable. Then, 75 mg $TiO_2$ or $NO_3^-/TiO_2$ powders were introduced and the concentration of HCHO decreased upon the introduction. It took about another 60 min for HCHO concentration to get stable. After the concentrations of both HCHO and aerosol became stable, the lamps were turned on and the concentrations of $NO_x$ were monitored.

To determine the background value of $NO_x$ in the reaction system, four blank experiments were carried out under illumination without nitrate: "synthetic air", "synthetic air + $TiO_2$", "synthetic air + HCHO" and "synthetic air + HCHO + $TiO_2$". In the blank experiments of "synthetic air" and "synthetic air + $TiO_2$", the $NO_x$ concentration remained stable during 180 min illumination, and the concentration change was no more than 0.5 ppb (Figure S4a). Therefore, the environmental chamber, synthetic air and the surface of $TiO_2$ particles were thought to be relatively clean, and there was no generation and accumulation of $NO_x$ under illumination. When HCHO

https://doi.org/10.5194/acp-2022-6
Preprint. Discussion started: 27 January 2022


Atmospheric Chemistry and Physics Discussions

was introduced into the environmental chamber, $NO_x$ accumulated ~2 ppb in 120 min with or without $TiO_2$ particles (Figure S4b). Compared with the blank experiment results when there was no HCHO, $NO_x$ might come from the generation process of HCHO (impurities in paraformaldehyde). However, considering the high concentration level of $NO_x$ produced in the $NO_3^-$-$TiO_2$ system containing HCHO under the same conditions in this study (see later in Figure 2), the $NO_x$ generated in this blank experiment can be negligible.

## 3 Results and discussion

### 3.1 The positive effect of $TiO_2$ on the renoxification process

We investigated the photocatalytic role of $TiO_2$ on renoxification. The light source was two 365 nm tube lamps containing small amounts of 400–600 nm visible light; this setup was suitable for exciting $TiO_2$ and the photolysis of available nitrate radicals. Raw $NO_x$ data measured in the chamber under dark and illuminated conditions for 4 wt.% $KNO_3$-$SiO_2$ and 4 wt.% $KNO_3$-$TiO_2$ (1 wt.%)/$SiO_2$ are shown in Figure 1. The ratio of 1 wt. % $TiO_2$ to $SiO_2$ corresponds to their ratio in sand and dust particles. We observed no $NO_x$ in the $KNO_3$-$SiO_2$ sample under dark or illumination, indicating very weak direct photolysis of nitrate under our 365 nm tube-lamp illumination conditions. However, when the sample containing $TiO_2$/$SiO_2$ was illuminated, $NO_x$ continually accumulated in the chamber. This finding confirms that $NO_x$ production arising from photodissociation of $NO_3^-$ on $TiO_2$/$SiO_2$ was caused by the photocatalytic property of $TiO_2$ (i.e., photocatalytic renoxification) and was not due to the direct photolysis of $NO_3^-$ (photolytic renoxification).

https://doi.org/10.5194/acp-2022-6
Preprint. Discussion started: 27 January 2022


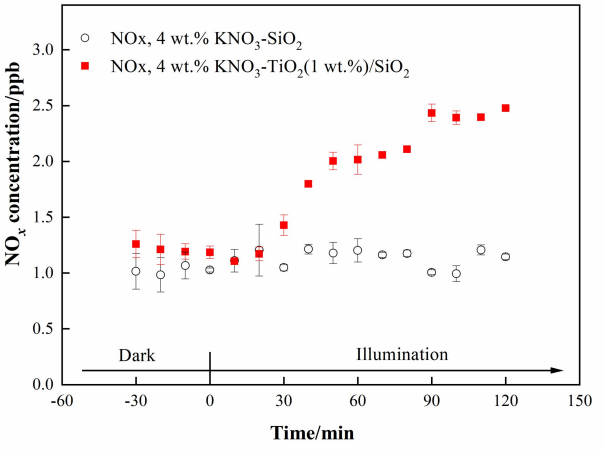


**Figure 1.** Effect of illumination on the release of $NO_x$ from 4 wt.% $KNO_3$-$SiO_2$ and 4 wt.% $KNO_3$-$TiO_2$(1 wt.%)/$SiO_2$ at 293 K and 0.8% of relative humidity. 365 nm tube lamps were used during the illumination experiments.

$TiO_2$ can be excited by UV illumination to generate electron-hole pairs, and the $h^+$ can react with adsorbed $NO_3^-$ to produce $NO_3\cdot$ (Ndour et al., 2009). Thus, in the present study, $NO_3\cdot$ mainly absorbed visible light emitted from the tube lamps, which was subsequently photolyzed to $NO_x$ through Eqs. (3) and (4) (Wayne et al., 1991), which explains why $NO_x$ was observed in this study. Thus, we demonstrated that $TiO_2$ can be excited at illumination wavelengths of ~365 nm, even when then content was very low, and that $NO_x$ accumulated due to the production and further phytolysis of $NO_3\cdot$. However, the production rate of $NO_x$ was very slow, reaching only 1.3 ppb during 90 min of illumination. This result may have been caused by the blocking effect of $K^+$ on $NO_3^-$. $K^+$ forms ion pairs with $NO_3^-$, and electrostatic repulsion between $K^+$ and $h^+$ prevents $NO_3^-$ from combining with $h^+$ to generate $NO_3\cdot$ to a certain extent, thereby weakening the positive effect of $TiO_2$ on the renoxification of

https://doi.org/10.5194/acp-2022-6
Preprint. Discussion started: 27 January 2022


Atmospheric Chemistry and Physics Discussions

$KNO_3$ (Rosseler et al., 2013).

$$TiO_2 + h\upsilon\ (\lambda < 390\ nm) \rightarrow e^- + h^+ \quad (1)$$

$$NO_3^- + h^+ \rightarrow NO_3\cdot \quad (2)$$

$$NO_3\cdot + h\upsilon\ (\lambda < 640\ nm) \rightarrow NO_2 + O\cdot \quad (3)$$

$$NO_3\cdot + h\upsilon\ (585\ nm < \lambda < 640\ nm) \rightarrow NO + O_2 \quad (4)$$

### 3.2 The synergistic positive effect of $TiO_2$ and HCHO on the renoxification process

LED lamps with a wavelength range of 350–390 nm and no visible light were used to irradiate 4 wt.% $KNO_3$-$TiO_2$ without generating $NO_x$ ($NO_2$ and NO concentrations fluctuate within the error range of the instrument) (Figure S5). $TiO_2$ can be excited under this range of irradiation, producing $NO_3$ radicals as discussed above. The lack of $NO_x$ generation indicates that neither nitrate photolysis nor $NO_3\cdot$ photolysis occurred under 365 nm LED lamp illumination conditions. In addition, it has been shown that $NO_3\cdot$ photolysis only occurs in visible light (Aldener et al., 2006). Therefore, the LED lamp setup was used in subsequent experiments to exclude the direct photolysis of both $KNO_3$ and $NO_3\cdot$, but allow the excitation of $TiO_2$. This approach allowed us to investigate the process of photocatalytic renoxification caused by HCHO in the presence of photogenerated $NO_3\cdot$.

Atmospheric trace gases can undergo photocatalytic reactions on the surface of $TiO_2$ (Chen et al., 2012). As the illumination time increased, the concentration of HCHO showed a linear downward trend, which was consistent with zero-order

https://doi.org/10.5194/acp-2022-6
Preprint. Discussion started: 27 January 2022


Atmospheric Chemistry and Physics Discussions

reaction kinetics (Figure S6). The zero-order reaction rate constants of HCHO on $TiO_2$ and 4 wt.% $KNO_3$-$TiO_2$ particles were 9.1 × $10^{-3}$ and 1.4 × $10^{-2}$ ppm $min^{-1}$, respectively, which were much higher than that for gaseous HCHO photolysis (Shang et al., 2017). We suggested that the produced $NO_3$· contributed to the enhanced uptake of HCHO. Therefore, we suggest that $NO_3$· production contributed to enhanced HCHO uptake. Future studies should explore whether HCHO affects the photocatalytic renoxification of $NO_3^-$-$TiO_2$.

Variation in $NO_x$ concentration within the chamber containing nitrate-$TiO_2$ particles with or without HCHO is shown in Figure 2. For $KNO_3$-$TiO_2$ particles, the $NO_x$ concentration began to increase upon irradiation in the presence of HCHO, reaching ~110 ppb within 120 min. This result indicates that HCHO greatly promoted photocatalytic renoxification of $KNO_3$ on the surfaces of $TiO_2$ particles. This reaction process can be divided into two stages: a rapid increase within the first 60 min and a slower increase within the following 60 min, each consistent with zero-order reaction kinetics. The slow stage is due to the photodegradation of HCHO on $KNO_3$-$TiO_2$ aerosols, which led to a decrease in its concentration, gradually weakening the positive effect. $NO_x$ is the sum of $NO_2$ and NO, both of which showed a two-stage concentration increase. The $NO_2$ generation rate was nearly 6 times that of NO, as compared to using the zero-order rate constant within 60 min (1.18 ppb $min^{-1}$ $NO_2$, $R^2$ = 0.96; 0.19 ppb $min^{-1}$ NO, $R^2$ = 0.91). This burst-like generation of $NO_x$ can be ascribed to the reaction between generated $NO_3$· and HCHO via hydrogen abstraction to form adsorbed nitric acid ($HNO_3$(ads)) on $TiO_2$ particles. Based on the analysis of

https://doi.org/10.5194/acp-2022-6
Preprint. Discussion started: 27 January 2022


Atmospheric Chemistry and Physics Discussions

the absorption cross section of $HNO_3$ adsorbed on fused silica surface，the $HNO_3$(ads) absorption spectrum has been reported to be red-shifted compared to $HNO_3$(g), extending from 350 to 365 nm, with a simultaneous cross-sectional increase (Du and Zhu, 2011). Therefore, $HNO_3$(ads) was subjected to photolysis to produce $NO_2$ and HONO (Eqs. (6)-(8)) under the LED lamp used in this study. A previous study of $HNO_3$ photolysis on the surface of Pyrex glass showed that the ratio of the formation rates of photolysis products ($J_{NOx}/J_{(NOx+HONO)}$) was > 97% at RH = 0% (Zhou et al., 2003), suggesting that $NO_x$ is the main gaseous product under dry conditions. Thus, the effect of HONO on product distribution and $NO_x$ concentration was negligible in this study. Together, these results suggest that $NO_3\cdot$ and HCHO generate $HNO_3$(ads) on particle surfaces through hydrogen abstraction, which contributes to the substantial release of $NO_x$ via photolysis. This photocatalytic renoxification via the $NO_3^-$-$NO_3\cdot$-HCHO-$HNO_3$-$NO_x$ pathway is important considering the high abundance of hydrogen donor organics in the atmosphere.

$$NO_3\cdot + HCHO \rightarrow CHO\cdot + HNO_3(ads) \quad (5)$$

$$HNO_3(ads) + h\upsilon \rightarrow [HNO_3]^*(ads) \quad (6)$$

$$[HNO_3]^*(ads) \rightarrow HNO_2(ads) + O(^3P)(ads) \quad (7)$$

$$[HNO_3]^*(ads) \rightarrow NO_2(ads) + \cdot OH(ads) \quad (8)$$

https://doi.org/10.5194/acp-2022-6
Preprint. Discussion started: 27 January 2022


Atmospheric Chemistry and Physics Discussions

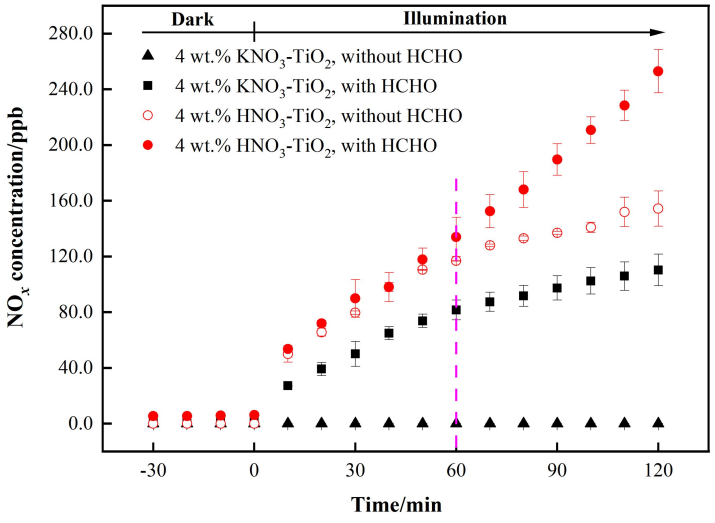


**Figure 2.** Effect of formaldehyde on the renoxification processes of different nitrate-doped particles at 293 K and 0.8% of relative humidity. 365 nm LED lamps were used during the illumination experiment. The initial concentration of HCHO was about 9 ppm.

To demonstrate the proposed HCHO mechanism and the photolysis contribution of $HNO_3$ to $NO_x$, we prepared an $HNO_3$-$TiO_2$ sample by directly dissolving $TiO_2$ into dilute nitric acid. The formation of $NO_x$ on $HNO_3$-$TiO_2$ without HCHO under illumination was obvious (Figure 2), and occurred even more rapidly than that on $KNO_3$-$TiO_2$ with HCHO. The renoxification of $HNO_3$-$TiO_2$ particles was further enhanced following the introduction of HCHO. The $NO_x$ concentration increased by ~250 ppb after 2 h of illumination, which was 2.2 times faster than the increase in $KNO_3$-$TiO_2$ concentration under the same conditions. This difference is due to the fact that $HNO_3$ dissociates on particle surfaces to generate $NO_3^-$, such that $HNO_3$ exists on $TiO_2$ as both $HNO_3$(ads) and $NO_3^-$(ads). Similarly, $NO_3^-$(ads) completed the

https://doi.org/10.5194/acp-2022-6
Preprint. Discussion started: 27 January 2022


Atmospheric Chemistry and Physics Discussions

285 $NO_3^-$-$NO_3$·-HCHO-$HNO_3$-$NO_x$ pathway as described above through the reaction
286 process shown in Eqs. (2) to (8). The rates of $NO_x$ production from $HNO_3$-$TiO_2$
287 particles with and without HCHO were similar for the first 60 min (Figure 2), mainly
288 due to the direct photolysis of partial $HNO_3$(ads). However, after 60 min, $NO_x$ was
289 generated rapidly in the presence of HCHO, perhaps due to the dominant
290 photocatalytic renoxification of $NO_3^-$(ads). These findings indicate that HCHO
291 converts $NO_3^-$ on particle surfaces into $HNO_3$(ads) by reacting with $NO_3$·, and then
292 $HNO_3$(ads) photolyzes at a faster rate to generate $NO_x$, allowing HCHO to enhance
293 the formation of $NO_x$. Overall, the photocatalytic renoxification of $NO_3^-$-$TiO_2$
294 particles affects atmospheric oxidation and the nitrogen cycle, and the presence of
295 HCHO further enhances this impact.

296 Photocatalytic renoxification reaction occurs on the surfaces of mineral dust due
297 to the presence of semiconductor oxides with photocatalytic activity such as $TiO_2$
298 (Ndour et al., 2009). In this study, we selected the commercial mineral dust ATD to
299 study the effects of HCHO on this process. We detected ·OH in irradiated pure $TiO_2$
300 and ATD samples using electron spin resonance (ESR) technique, and found that for
301 ATD samples, the peak intensity of ·OH generation was 40% that of $TiO_2$ samples
302 (Figure S8). ·OH originates in the reaction of $h^+$ with surface adsorbed water (Ahmed
303 et al., 2014). ATD contains semiconductor oxides such as $TiO_2$ and $Fe_2O_3$, and is
304 thought to exhibit photocatalytic properties affecting the renoxification of nitrate. The
305 $NO_3^-$ content of ATD is $4 \times 10^{17}$ molecules $m^{-2}$, which is ~0.25 wt.% of the total mass
306 (Huang et al., 2015; Jiyeon et al., 2017). The $NO_x$ concentration changes observed in

https://doi.org/10.5194/acp-2022-6
Preprint. Discussion started: 27 January 2022


Atmospheric Chemistry and Physics Discussions

the environmental chamber demonstrated that HCHO promoted the renoxification of ATD particles (Figure S9). This result suggests that mineral dust containing photocatalytic semiconductor oxides such as $TiO_2$, $Fe_2O_3$, and ZnO can greatly promote the conversion of granular nitrate to $NO_x$ in the presence of HCHO.

### 3.3 Influential factors on the photocatalytic renoxification process

#### 3.3.1 The influence of nitrate type

As discussed above, $HNO_3$ and $KNO_3$ undergo different renoxification processes on the surface of $TiO_2$ under the same illumination conditions, suggesting that cations bound to $NO_3^-$ significantly affect $NO_x$ production. Different types of cations coexist with nitrate ions in atmospheric particulate matter, among which ammonium ions ($NH_4^+$) are important water-soluble ions that can be higher in content than $K^+$ in urban fine particulate matter (Zhou et al., 2016; Tang et al., 2021; Wang et al., 2021), especially in heavily polluted cities.(Tian et al., 2020) Equal amounts of 4 wt.% $NH_4NO_3$-$TiO_2$ particles were introduced into the chamber and illuminated under the same conditions. HCHO had a much stronger positive effect on the release of $NO_x$ over $NH_4NO_3$-$TiO_2$ particles (Figure 3), which may be ascribed to $NH_4^+$. Combined with the results of $NH_4NO_3$-$TiO_2$ particles and $KNO_3$-$TiO_2$ particles, it seems that the affinity rather than electrostatic repulsion should be the primary effect of cations on the production of $NO_x$. On substrates without photocatalytic activity such as $SiO_2$ and $Al_2O_3$, $NH_4NO_3$ cannot generate $NO_x$,(Ma et al., 2021) such that $NO_x$ production depends on the effect of $TiO_2$. The $h^+$ generated by $TiO_2$ excitation reacts with adsorbed $H_2O$ to produce ·OH (Eq. (9)), which gradually oxidizes $NH_4^+$ to $NO_3^-$ (Eq.

https://doi.org/10.5194/acp-2022-6
Preprint. Discussion started: 27 January 2022


Atmospheric Chemistry and Physics Discussions

329 (10)). In our previous study, we demonstrated that irradiated $(NH_4)_2SO_4$-$TiO_2$ samples
330 had lower $NH_4^+$ and $NO_3^-$ peaks (Shang et al., 2017). Therefore, more $NO_3^-$
331 participated in the photocatalytic renoxification process via the
332 $NO_3^-$-$NO_3$·-HCHO-$HNO_3$-$NO_x$ pathway to generate $NO_x$. Moreover, the results
333 without HCHO are shown in Figure 4a, both $NH_4NO_3$-$TiO_2$ particles and $KNO_3$-$TiO_2$
334 particles produced almost no $NO_x$, indicating the importance of HCHO for
335 renoxification to occur. Due to the high content of $NH_4NO_3$ in atmospheric particulate
336 matter, the positive effect of HCHO on the photocatalytic renoxification process may
337 have some impact on the concentrations of $NO_x$ and other atmospheric oxidants.

$$h^+ + H_2O \rightarrow \cdot OH \quad (9)$$

338

$$\cdot OH + NH_4^+ / NH_3 \rightarrow NO_2^- \rightarrow NO_3^- \quad (10)$$

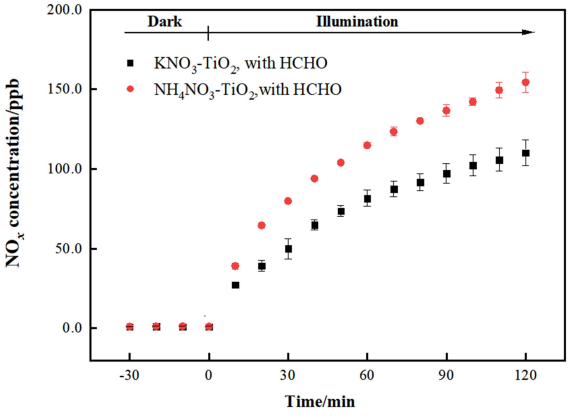


339

340 **Figure 3.** Effect of formaldehyde on the renoxification processes of 4 wt.%
341 $NH_4NO_3$-$TiO_2$ and 4 wt.% $KNO_3$-$TiO_2$ particles at 293 K and 0.8% of relative
342 humidity. 365 nm LED lamps were used during the irradiation experiment. The initial
343 concentration of HCHO was about 9 ppm.

344

https://doi.org/10.5194/acp-2022-6
Preprint. Discussion started: 27 January 2022


Atmospheric Chemistry and Physics Discussions

### 3.3.2 The influence of nitrate content

Atmospheric particles have a wide range of nitrate content; differences in the relative amounts of nitrate and $TiO_2$ in atmospheric particles may affect the renoxification process. Therefore, we investigated the effects of nitrate concentration gradients on renoxification. Changes in the $NO_x$ concentrations of $NO_3^-$-$TiO_2$ composite particles, with or without HCHO, according to reaction time under 365 nm LED illumination confirmed zero-order reaction kinetics. Therefore, we applied zero-order rate constants to compare particles with different nitrate contents. For $KNO_3$-$TiO_2$, $NO_x$ was not generated in the absence of HCHO, even at high $NO_3^-$ nitrate concentrations (Figure 4a) because no photolysis of either $NO_3^-$ or the $NO_3$ radical occurred under 365 nm LED illumination. For $NH_4NO_3$-$TiO_2$, the rate of $NO_x$ generation increased in the absence of HCHO as $NH_4NO_3$ content increased, and at higher levels (80 and 95 wt.%), the $NO_x$ generation rate constant reached a plateau at ~$8.0 \times 10^{-2}$ ppb $min^{-1}$ because both $NH_4^+$ and NO are photochemically oxidized on $TiO_2$ to generate $NO_3^-$, and part of this NO was oxidized to $NO_2$ by $O_2$.(Ma et al., 2021) Higher $NO_3^-$ content leads to higher $NH_4^+$ concentration; thus, more $NH_4^+$ participated in the generation of $NO_x$ through photooxidation. When $NO_3^-$ content reached 80 wt.% or higher, limited $TiO_2$ content in the chamber led to the saturation of $NH_4^+$ photooxidation, preventing further $NO_x$ generation. $NO_x$ release rates over $NO_3^-$-$TiO_2$ as nitrate content increased in the presence of HCHO are shown in Figure 4b. The $NO_x$ production rate first increased and then decreased, with a maximum of 4 wt.% nitrate content among both $KNO_3$-$TiO_2$ and $NH_4NO_3$-$TiO_2$ particles. This increasing trend was caused by the

https://doi.org/10.5194/acp-2022-6
Preprint. Discussion started: 27 January 2022


Atmospheric Chemistry and Physics Discussions

increased opportunities for contact between $TiO_2$ and $NO_3^-$ as nitrate content increased, which facilitated the combination of $h^+$ with $NO_3^-$ to form $NO_3\cdot$. The trend began to decrease when nitrate content exceeded 4 wt.%. Higher $NO_3^-$ content hindered reactions on the surface of $TiO_2$, but rapidly decreased the Brunauer, Emmett and Teller (BET) surface area of the composite particles (Shang et al., 2017), which weakened HCHO uptake and particle surface reactions. The amount of $NO_x$ produced by $NH_4NO_3$-$TiO_2$ was consistently higher than that of $KNO_3$-$TiO_2$. The possible reasons for this difference are as follows. First, like the $K^+$ blocking effect discussed in section 3.1, $NO_3\cdot$ generated from the reaction of $NO_3^-$ with $h^+$ was weakened; thus, little adsorbed $HNO_3$ was available for further renoxification. Additionally, $NH_4^+$ can undergo a photooxidation reaction to generate more $NO_x$ by $TiO_2$, as occurs in the absence of HCHO.

https://doi.org/10.5194/acp-2022-6
Preprint. Discussion started: 27 January 2022


Atmospheric Chemistry and Physics Discussions

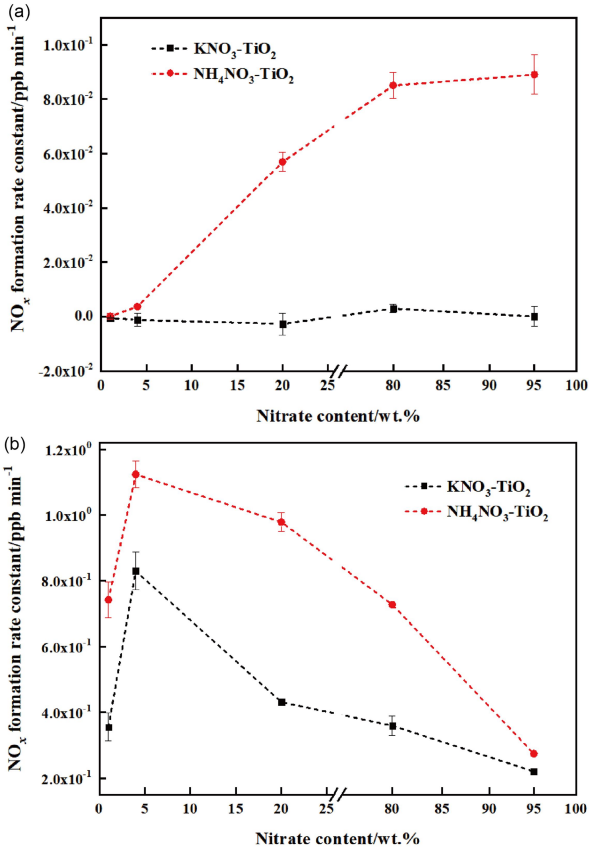


379

380 **Figure 4.** Effect of nitrate content (1 wt.%, 4 wt.%, 20 wt.%, 80 wt.% and 95 wt.%)
381 on the release of $NO_x$ for $NH_4NO_3$-$TiO_2$ and $KNO_3$-$TiO_2$ at 293 K and 0.8% of
382 relative humidity. 365 nm LED lamps were used during the illumination experiment.
383 (a) without HCHO; (b) the initial concentration of HCHO was about 9 ppm.

384 **3.3.3 The influence of relative humidity**

385 Water on particle surfaces can participate directly in the heterogeneous reaction
386 process. As shown in Eq. (9), $H_2O$ is captured by $h^+$ to generate ·OH with strong
387 oxidizability in photocatalytic reactions. The first-order photolysis rate constant of
388 $NO_3^-$ on $TiO_2$ particles decreases by an order of magnitude, from $(5.7 \pm 0.1) \times 10^{-4}$

https://doi.org/10.5194/acp-2022-6
Preprint. Discussion started: 27 January 2022


Atmospheric Chemistry and Physics Discussions

$s^{-1}$ on dry surfaces to $(7.1 \pm 0.8) \times 10^{-5}$ $s^{-1}$ when nitrate is coadsorbed with water above monolayer coverage (Ostaszewski et al., 2018). We explored the positive effect of HCHO on the $NO_3^-$-$TiO_2$ particle photocatalytic renoxification at different RH levels; the results are shown in Figure 5a. For $KNO_3$-$TiO_2$ particles, the rate of $NO_x$ production decreased as the RH of the environmental chamber increased, indicating that increased water content in the gas phase hindered photocatalytic renoxification for two reasions: $H_2O$ competes with $NO_3^-$ for $h^+$ on the surface of $TiO_2$ to generate ·OH, reducing the generation of $NO_3$·, and competitive adsorption between $H_2O$ and HCHO causes the generated ·OH to compete with $NO_3$· for HCHO, hindering the formation of $HNO_3$(ads) on particle surfaces. Moreover, it is also possible that the loss of $NO_x$ on the wall increases under high humidity conditions, resulting in a decrease in its concentration. This competitive process also occurs on the surface of $NH_4NO_3$-$TiO_2$ particles, but at RH = 70%, the $NO_x$ generation rate constant is slightly higher. The deliquescent humidity of $NH_4NO_3$ at 298 K is ~62%, such that $NH_4NO_3$ had already deliquesced at RH = 70%, forming an $NH_4^+/NH_3$-$NO_3^-$ liquid system on the particle surfaces. This quasi-liquid phase improved the dispersion of $TiO_2$ in $NH_4NO_3$, resulting in greater $NO_x$ release. The deliquescent humidity of $KNO_3$-$TiO_2$ was > 90%,(2009) such that no phase change occurred at RH = 70%, and the renoxification reaction rate retained a downward trend. In the presence of $H_2O$, in addition to the $NO_3^-$-$NO_3$·-HCHO-$HNO_3$ pathway observed in this study, there are a variety of $HNO_3$ generation paths, such as the hydrolysis of $N_2O_5$ via the $NO_2$-$N_2O_5$-$HNO_3$ pathway (Brown et al., 2005), the

https://doi.org/10.5194/acp-2022-6
Preprint. Discussion started: 27 January 2022


Atmospheric Chemistry and Physics Discussions

411 oxidation of $NO_2$ by ·OH (Burkholder et al., 1993), and the reaction of $NO_3$· with
412 $H_2O$ (Schutze and Herrmann, 2005), all of which require further consideration and
413 study.

414 The formation rates of NO and $NO_2$ are shown in Figure 5b and c, respectively.
415 $NO_2$ was the main product of surface $HNO_3$ photolysis. Under humid conditions,
416 generated $NO_2$(ads) continued to react with $H_2O$ adsorbed on the surface to form
417 HONO(ads). HONO was desorbed from the surface and released into the gas phase
418 (Zhou et al., 2003; Bao et al., 2018; Pandit et al., 2021), providing gaseous HONO to
419 the reaction system. Because the $NO_x$ concentration remained high, the effect of
420 HONO on $NO_x$ analyzer results was negligible (Shi et al., 2021a). As $NO_2$ can form
421 $NO_2^-$ with $e^-$, a reverse reaction also occurred between $NO_2^-$ and HONO in the
422 presence of $H_2O$ (Ma et al., 2021; Garcia et al., 2021). Therefore, the increase in $H_2O$
423 increased the proportion of HONO in the nitrogen-containing products, such that the
424 $NO_x$ generation rate decreased as RH increased. Comparing Figure 5b and c shows
425 that, as RH increased, the NO production rate constant decreased more than that of
426 $NO_2$. HONO and $NO_2$ generated by the photolysis of $HNO_3$(ads) decreased
427 accordingly, i.e., the NO source decreased. However, generated $NO_2$ and NO
428 underwent photocatalytic oxidation on the surface of $TiO_2$, and NO photodegradation
429 was more significant under the same conditions (Hot et al., 2017). Generally, a certain
430 amount of HONO will be generated during the reaction between HCHO and
431 $NO_3^-$-$TiO_2$ particles when RH is high, which affects the concentrations of
432 atmospheric ·OH, $NO_x$, and $O_3$. This process is more likely to occur in summer due to

https://doi.org/10.5194/acp-2022-6
Preprint. Discussion started: 27 January 2022


Atmospheric Chemistry and Physics Discussions

433 high RH and light intensity affecting atmospheric oxidation. In drier winters or dusty
434 weather, when $TiO_2$ content is high, HCHO greatly promotes the photocatalytic
435 renoxification of $NO_3^-$-$TiO_2$ particles, thereby releasing more $NO_x$ into the
436 atmosphere, affecting the global atmospheric nitrogen budget. Thus, regardless of the
437 seasonal and regional changes, renoxification has significant practical importance.

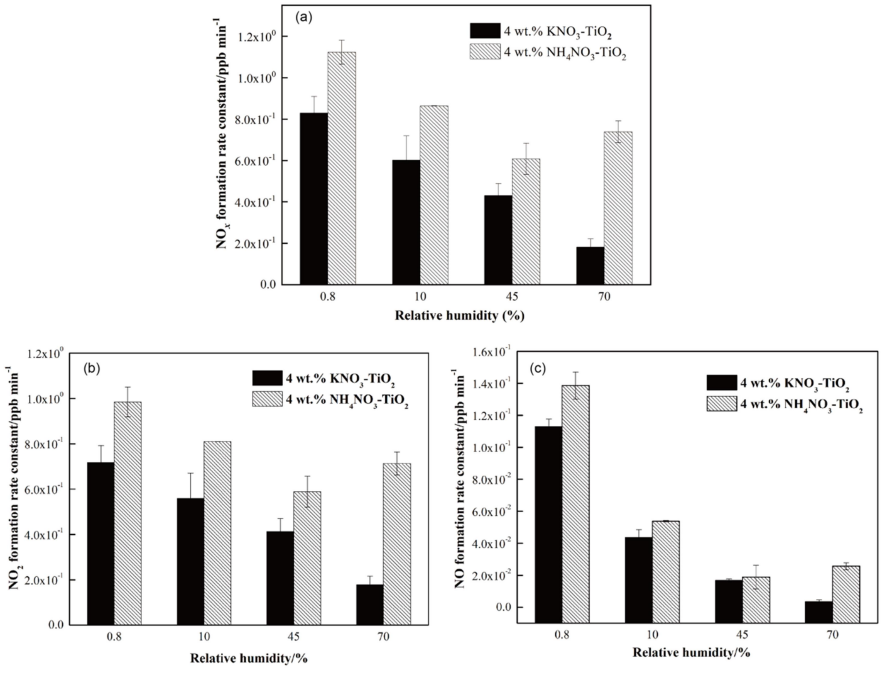


438

439 **Figure 5.** Effect of relative humidity on the release of $NO_x$ (a), $NO_2$ (b), NO (c) over 4
440 wt.% $NH_4NO_3$-$TiO_2$ and 4 wt.% $KNO_3$-$TiO_2$ particles at 293 K. 365 nm LED lamps
441 were used during the illumination experiment. The initial concentration of HCHO was
442 about 9 ppm.

443 **3.3.4 The influence of initial HCHO concentration**

444 To explore whether HCHO promotes nitrate renoxification at natural concentration
445 levels, we reduced the initial concentration of HCHO in the environmental chamber

https://doi.org/10.5194/acp-2022-6
Preprint. Discussion started: 27 January 2022


Atmospheric Chemistry and Physics Discussions

by a factor of 10, to ~1.0 ppm. The positive effect of HCHO on the photocatalytic renoxification of $KNO_3$-$TiO_2$ particles was clearly weakened, with $NO_2$ concentration first increasing and then decreasing, and NO concentration remaining stable (Figure S10). The HCHO concentration decreased due to its consumption during the reaction, making its positive effect decline quickly. The photocatalytic oxidation reaction between $NO_x$ and photogenerated reactive oxygen species (ROS) on the $TiO_2$ surface further decreased the $NO_x$ concentration. Photocatalytic oxidation of $NO_x$ by ROS on $TiO_2$ particles occurred at an HCHO concentration of 9 ppm, but the positive effect of HCHO remained dominant. Thus, no decrease in $NO_x$ concentration was observed within 120 min in our experiments.

The concentration of HCHO in the atmosphere is relatively low, with a balance between the photocatalytic oxidation decay of $NO_x$ and the release of $NO_x$ via photocatalytic renoxification. The mutual transformation between particulate $NO_3^-$ and gaseous $NO_x$ is more complex. The effect of low-concentration HCHO on the renoxification of $NO_3^-$-$TiO_2$ particles requires further investigation. However, many types of organics provide hydrogen atoms in the atmosphere, including alkanes (e.g., methane and n-hexane), aldehydes (e.g., acetaldehyde), alcohols (e.g., methanol and ethanol), and aromatic compounds (e.g., phenol) that react with $NO_3\cdot$ to produce nitric acid (Atkinson, 1991). These organics, together with HCHO, play similar positive roles in photocatalytic renoxification and, therefore, influence $NO_x$ concentrations.

## 4 Atmospheric implications

Nitric acid and nitrate are not only the final sink of $NO_x$ in the atmosphere but

https://doi.org/10.5194/acp-2022-6
Preprint. Discussion started: 27 January 2022


Atmospheric Chemistry and Physics Discussions

are also among its important sources. $NO_x$ from nitrate through renoxification is easily overlooked. The renoxification of nitrate on the surface of $TiO_2$ particles can be divided into photolytic renoxification and photocatalytic renoxification. The photocatalytic performance of $TiO_2$ promotes the renoxification process, which explains the influence of semiconducting metal oxide components on atmospheric mineral particles during the renoxification of nitrate. Although most previous studies have focused on solid-phase nitrate renoxification, our exploration of the roles of HCHO in this study will allow us to examine complex real-world pollution scenarios, in which multiple atmospheric pollutants coexist, as well as the effects of organic pollutants on the renoxification process. Atmospheric HCHO is taken up at the surface of particulate matter, accounting for up to ~50% of its absorption (Li et al., 2014), such that the heterogeneous participation of HCHO during renoxification is important. This study is the first to report that HCHO has a positive effect on the photocatalytic renoxification of nitrate on $TiO_2$ particles, via the $NO_3^-$-$NO_3$·-HCHO-$HNO_3$-$NO_x$ pathway (Figure 6), further increasing the release of $NO_x$ and other nitrogen-containing active species, which in turn affects the photochemical cycle of $HO_x$ radicals in the atmosphere and the formation of important atmospheric oxidants such as $O_3$. Factors such as particulate matter composition, RH, and initial HCHO concentration all influence the positive effect of HCHO; notably, $H_2O$ competes with $NO_3^-$ for photogenerated holes. Based on these findings, two balance systems should be explored in depth: the influence of RH on the generation rates of HONO and $NO_x$, as water increases the proportion of HONO in

https://doi.org/10.5194/acp-2022-6
Preprint. Discussion started: 27 January 2022


Atmospheric Chemistry and Physics Discussions

490 nitrogen-containing products; and the balance between the photocatalytic degradation
491 of generated $NO_x$ on $TiO_2$ particles and the positive effect of HCHO on $NO_x$
492 generation at low HCHO concentrations.

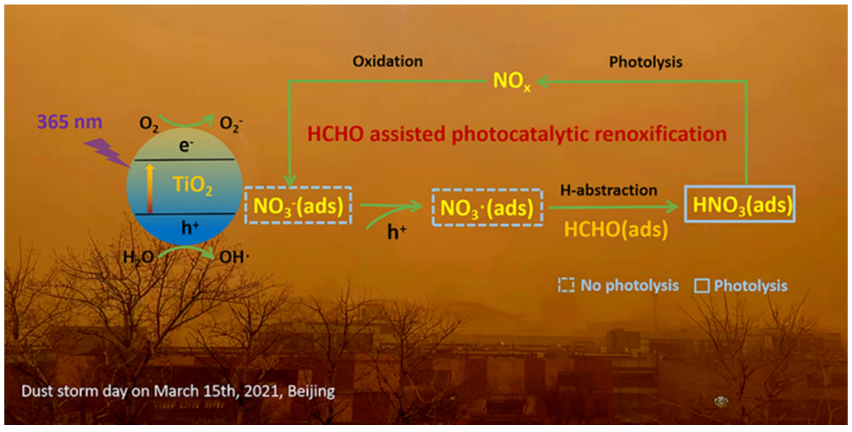


493

494 **Figure 6.** Positive role of HCHO on the photocatalytic renoxification of nitrate-$TiO_2$
495 composite particles via the $NO_3^-$-$NO_3$·-HCHO-$HNO_3$-$NO_x$ pathway.

496 Based on our results, we conclude that in photochemical processes on the
497 surfaces of particles containing semiconductor oxides, with the participation of
498 hydrogen donor organics, a significant synergistic photocatalytic renoxification
499 enhancement effect alters the composition of surface nitrogenous species via the
500 $NO_3^-$-$NO_3$·-hydrogen donor-$HNO_3$-$NO_x$ pathway, thereby affecting atmospheric
501 oxidation and nitrogen cycling. The positive effect of HCHO can be extended from
502 $TiO_2$ in this study to other components of mineral dust such as $Fe_2O_3$ and ZnO with
503 photocatalytic activity, which may have practical applications. Our proposed reaction
504 mechanism by which HCHO promotes photocatalytic renoxification will improve
505 existing atmospheric chemistry models and reduce discrepancies between model
506 simulations and field observations.

https://doi.org/10.5194/acp-2022-6
Preprint. Discussion started: 27 January 2022


Atmospheric Chemistry and Physics Discussions

507

508 ***Supplement.***

509 Detailed information of Figures S1-10 (which include the spectra of the lamps,
510 size distribution of $TiO_2$ particles and changes of HCHO concentration in
511 environmental chamber, changes of $NO_x$ concentration under different reaction
512 conditions, photodegradation curve of HCHO, ESR spectra of $TiO_2$ and ATD
513 particles), and Table S1 (which demonstrate ATD chemical composition) .

514

515 ***Acknowledgments***

516 The authors are grateful to the financial support provided by National Natural
517 Science Foundation of China (Nos. 21876003, 41961134034 and 21277004), the
518 Second Tibetan Plateau Scientific Expedition and Research (No. 2019QZKK0607),
519 and the 111 Project Urban Air Pollution and Health Effects (B20009).

520

521 **References**

522 Ahmed, A. Y., Kandiel, T. A., Ivanova, I., and Bahnemann, D.: Photocatalytic and
523 photoelectrochemical oxidation mechanisms of methanol on $TiO_2$ in aqueous solution,
524 Appl.Surf. Sci., 319, 44-49, 10.1016/j.apsusc.2014.07.134, 2014.
525 Aldener, M., Brown, S. S., Stark, H., Williams, E. J., Lerner, B. M., Kuster, W. C.,
526 Goldan, P. D., Quinn, P. K., Bates, T. S., Fehsenfeld, F. C., and Ravishankara, A. R.:
527 Reactivity and loss mechanisms of $NO_3$ and $N_2O_5$ in a polluted marine environment:
528 Results from in situ measurements during New England Air Quality Study 2002, J.
529 Geophys. Res-Atmos., 111, 10.1029/2006jd007252, 2006.
530 Alexander, B., Sherwen, T., Holmes, C. D., Fisher, J. A., Chen, Q., Evans, M. J., and
531 Kasibhatla, P.: Global inorganic nitrate production mechanisms: comparison of a

https://doi.org/10.5194/acp-2022-6
Preprint. Discussion started: 27 January 2022


532 global model with nitrate isotope observations, Atmos. Chem. Phys., 20, 3859-3877,
533 10.5194/acp-20-3859-2020, 2020.
534 Atkinson, R.: Kinetics and mechanisms of the gas-phase reactions of the $NO_3$ radical
535 with organic-comounds, J. Phys. and Chem. Ref. Data, 20, 459-507,
536 10.1063/1.555887, 1991.
537 Baergen, A. M. and Donaldson, D. J.: Photochemical Renoxification of Nitric Acid on
538 Real Urban Grime, Environ. Sci. Technol., 47, 815-820, 10.1021/es3037862, 2013.
539 Bao, F., Li, M., Zhang, Y., Chen, C., and Zhao, J.: Photochemical Aging of Beijing
540 Urban $PM_{2.5}$: HONO Production, Environ. Sci. Technol., 52, 6309-6316,
541 10.1021/acs.est.8b00538, 2018.
542 Bao, F., Jiang, H., Zhang, Y., Li, M., Ye, C., Wang, W., Ge, M., Chen, C., and Zhao, J.:
543 The Key Role of Sulfate in the Photochemical Renoxification on Real $PM_{2.5}$, Environ.
544 Sci. Technol., 54, 3121-3128, 10.1021/acs.est.9b06764, 2020.
545 Bedjanian, Y. and El Zein, A.: Interaction of $NO_2$ with $TiO_2$ Surface Under UV
546 Irradiation: Products Study, J. Phys. Chem. A, 116, 1758-1764, 10.1021/jp210078b,
547 2012.
548 Brown, S. S., Osthoff, H. D., Stark, H., Dube, W. P., Ryerson, T. B., Warneke, C., de
549 Gouw, J. A., Wollny, A. G., Parrish, D. D., Fehsenfeld, F. C., and Ravishankara, A. R.:
550 Aircraft observations of daytime $NO_3$ and $N_2O_5$ and their implications for
551 tropospheric chemistry, J. Photochem. Photobio. A, 176, 270-278,
552 10.1016/j.jphotochem.2005.10.004, 2005.
553 Burkholder, J. B., Talukdar, R. K., Ravishankara, A. R., and Solomon, S.:
554 Temperature-dependence of the $HNO_3$ UV absorption cross-sections. J.
555 Geophys.Res-Atmos., 98, 22937-22948, 10.1029/93jd02178, 1993.
556 Chen, H., Nanayakkara, C. E., and Grassian, V. H.: Titanium Dioxide Photocatalysis
557 in Atmospheric Chemistry, Chem. Rev., 112, 5919-5948, 10.1021/cr3002092, 2012.
558 Deng, J. J., Wang, T. J., Liu, L., and Jiang, F.: Modeling heterogeneous chemical
559 processes on aerosol surface, Particuology, 8, 308-318, 10.1016/j.partic.2009.12.003,
560 2010.
561 Dentener, F. J. and Crutzen, P. J.: Reaction of $N_2O_5$ on tropospheric aerosols-impact

https://doi.org/10.5194/acp-2022-6
Preprint. Discussion started: 27 January 2022


562 on the global distributions od $NO_x$, $O_3$, and OH. J. Geophys. Res-Atmos., 98,
563 7149-7163, 10.1029/92jd02979, 1993.
564 Du, J. and Zhu, L.: Quantification of the absorption cross sections of surface-adsorbed
565 nitric acid in the 335-365 nm region by Brewster angle cavity ring-down spectroscopy,
566 Chem. Phys. Lett., 511, 213-218, 10.1016/j.cplett.2011.06.062, 2011.
567 Finlayson-Pitts, B. J. and Pitts, J. J. N.: Chemistry of the Upper and Lower
568 Atmosphere: Theory, Experiments and Applications, Academic Press1999.
569 Garcia, S. L. M., Pandit, S., Navea, J. G., and Grassian, V. H.: Nitrous Acid (HONO)
570 Formation from the Irradiation of Aqueous Nitrate Solutions in the Presence of
571 Marine Chromophoric Dissolved Organic Matter: Comparison to Other Organic
572 Photosensitizers, Acs Earth and Space Chem., 5, 3056-3064,
573 10.1021/acsearthspacechem.1c00292, 2021.
574 George, C., Ammann, M., D'Anna, B., Donaldson, D. J., and Nizkorodov, S. A.:
575 Heterogeneous Photochemistry in the Atmosphere, Chem. Rev., 115, 4218-4258,
576 10.1021/cr500648z, 2015.
577 Goodman, A. L., Bernard, E. T., and Grassian, V. H.: Spectroscopic study of nitric
578 acid and water adsorption on oxide particles: Enhanced nitric acid uptake kinetics in
579 the presence of adsorbed water, J. Phys. Chem. A, 105, 6443-6457,
580 10.1021/jp0037221, 2001.
581 Harris, G. W., Carter, W. P. L., Winer, A. M., Pitts, J. N., Platt, U., and Perner, D.:
582 Observations of nitrous-acid in the los-angeles atmosphere and implications for
583 predictions of ozone precursor relationships. Environ. Sci. Technol., 16, 414-419,
584 10.1021/es00101a009, 1982.
585 Hot, J., Martinez, T., Wayser, B., Ringot, E., and Bertron, A.: Photocatalytic
586 degradation of $NO/NO_2$ gas injected into a 10 $m^3$ experimental chamber, Environ. Sci.
587 Pollut. R., 24, 12562-12570, 10.1007/s11356-016-7701-2, 2017.
588 Huang, L., Zhao, Y., Li, H., and Chen, Z.: Kinetics of Heterogeneous Reaction of
589 Sulfur Dioxide on Authentic Mineral Dust: Effects of Relative Humidity and
590 Hydrogen Peroxide, Environ. Sci. Technol., 49, 10797-10805,
591 10.1021/acs.est.5b03930, 2015.

https://doi.org/10.5194/acp-2022-6
Preprint. Discussion started: 27 January 2022


592 Jiyeon, Park, Myoseon, Jang, Zechen, and Yu: Heterogeneous Photo-oxidation of $SO_2$
593 in the Presence of Two Different Mineral Dust Particles: Gobi and Arizona Dust,
594 Environ. Sci. Technol., 2017.
595 Kasibhatla, P., Sherwen, T., Evans, M. J., Carpenter, L. J., Reed, C., Alexander, B.,
596 Chen, Q., Sulprizio, M. P., Lee, J. D., Read, K. A., Bloss, W., Crilley, L. R., Keene, W.
597 C., Pszenny, A. A. P., and Hodzic, A.: Global impact of nitrate photolysis in sea-salt
598 aerosol on $NO_x$, OH, and $O_3$ in the marine boundary layer, Atmos. Chem. Phys., 18,
599 11185-11203, 10.5194/acp-18-11185-2018, 2018.
600 Kim, W.-H., Song, J.-M., Ko, H.-J., Kim, J. S., Lee, J. H., and Kang, C.-H.:
601 Comparison of Chemical Compositions of Size-segregated Atmospheric Aerosols
602 between Asian Dust and Non-Asian Dust Periods at Background Area of Korea, B.
603 Korean Chem. Soc., 33, 3651-3656, 10.5012/bkcs.2012.33.11.3651, 2012.
604 Lee, J. D., Moller, S. J., Read, K. A., Lewis, A. C., Mendes, L., and Carpenter, L. J.:
605 Year-round measurements of nitrogen oxides and ozone in the tropical North Atlantic
606 marine boundary layer, J. Geophys. Res-Atmos., 114, 10.1029/2009jd011878, 2009.
607 Lesko, D. M. B., Coddens, E. M., Swomley, H. D., Welch, R. M., Borgatta, J., and
608 Navea, J. G.: Photochemistry of nitrate chemisorbed on various metal oxide surfaces,
609 Phys. Chem. Chem. Phys., 17, 20775-20785, 10.1039/c5cp02903a, 2015.
610 Li, L., Wang, Q., Zhang, X., She, Y., Zhou, J., Chen, Y., Wang, P., Liu, S., Zhang, T.,
611 Dai, W., Han, Y., and Cao, J.: Characteristics of single atmospheric particles in a
612 heavily polluted urban area of China: size distributions and mixing states, Environ.
613 Sci. Pollut. R., 26, 11730-11742, 10.1007/s11356-019-04579-3, 2019.
614 Li, X., Rohrer, F., Brauers, T., Hofzumahaus, A., Lu, K., Shao, M., Zhang, Y. H., and
615 Wahner, A.: Modeling of HCHO and CHOCHO at a semi-rural site in southern China
616 during the PRIDE-PRD2006 campaign, Atmos. Chem. Phys., 14, 12291-12305,
617 10.5194/acp-14-12291-2014, 2014.
618 Linsebigler, A. L., Lu, G. Q., and Yates, J. T.: hotocatalysis on $TiO_2$
619 surfaces-principles, mechanisms, and selected results, Chem. Rev., 95, 735-758,
620 10.1021/cr00035a013, 1995.
621 Ma, Q., Zhong, C., Ma, J., Ye, C., Zhao, Y., Liu, Y., Zhang, P., Chen, T., Liu, C., Chu,

https://doi.org/10.5194/acp-2022-6
Preprint. Discussion started: 27 January 2022


Atmospheric Chemistry and Physics Discussions

622 B., and He, H.: Comprehensive Study about the Photolysis of Nitrates on Mineral
623 Oxides, Environ. Sci. Technol., 55, 8604-8612, 10.1021/acs.est.1c02182, 2021.
624 Monge, M. E., D"Anna, B., and George, C.: Nitrogen dioxide removal and nitrous
625 acid formation on titanium oxide surfaces--an air quality remediation process? Phys.
626 Chem. Chem. Phys., 12, 8991-8998, 2010.
627 Ndour, M., Conchon, P., D'Anna, B., Ka, O., and George, C.: Photochemistry of
628 mineral dust surface as a potential atmospheric renoxification process, Geophysical
629 Research Letters, 36, 4, 10.1029/2008gl036662, 2009.
630 Ninneman, M., Lu, S., Zhou, X. L., and Schwab, J.: On the Importance of
631 Surface-Enhanced Renoxification as an Oxides of Nitrogen Source in Rural and
632 Urban New York State, Acs Earth and Space Chem., 4, 1985-1992,
633 10.1021/acsearthspacechem.0c00185, 2020.
634 Ostaszewski, C. J., Stuart, N. M., Lesko, D. M. B., Kim, D., Lueckheide, M. J., and
635 Navea, J. G.: Effects of Coadsorbed Water on the Heterogeneous Photochemistry of
636 Nitrates Adsorbed on $TiO_2$, J. Phys. Chem. A, 122, 6360-6371,
637 10.1021/acs.jpca.8b04979, 2018.
638 Pandit, S., Garcia, S. L. M., and Grassian, V. H.: HONO Production from Gypsum
639 Surfaces Following Exposure to $NO_2$ and $HNO_3$: Roles of Relative Humidity and
640 Light Source, Environ. Sci. Technol., 55, 9761-9772, 10.1021/acs.est.1c01359, 2021.
641 Platt, U., Perner, D., Harris, G. W., Winer, A. M., and Pitts, J. N.: Observations of
642 nitrous-acid in an urban atmosphere by differential optical-absorption, Nature, 285,
643 312-314, 10.1038/285312a0, 1980.
644 Read, K. A., Mahajan, A. S., Carpenter, L. J., Evans, M. J., Faria, B. V. E., Heard, D.
645 E., Hopkins, J. R., Lee, J. D., Moller, S. J., Lewis, A. C., Mendes, L., McQuaid, J. B.,
646 Oetjen, H., Saiz-Lopez, A., Pilling, M. J., and Plane, J. M. C.: Extensive
647 halogen-mediated ozone destruction over the tropical Atlantic Ocean, Nature, 453,
648 1232-1235, 10.1038/nature07035, 2008.
649 Reed, C., Evans, M. J., Crilley, L. R., Bloss, W. J., Sherwen, T., Read, K. A., Lee, J.
650 D., and Carpenter, L. J.: Evidence for renoxification in the tropical marine boundary
651 layer, Atmos. Chem. Phys., 17, 4081-4092, 10.5194/acp-17-4081-2017, 2017.

https://doi.org/10.5194/acp-2022-6
Preprint. Discussion started: 27 January 2022


Atmospheric Chemistry and Physics Discussions

652 Romer, P. S., Wooldridge, P. J., Crounse, J. D., Kim, M. J., Wennberg, P. O., Dibb, J.
653 E., Scheuer, E., Blake, D. R., Meinardi, S., Brosius, A. L., Thames, A. B., Miller, D.
654 O., Brune, W. H., Hall, S. R., Ryerson, T. B., and Cohen, R. C.: Constraints on
655 Aerosol Nitrate Photolysis as a Potential Source of HONO and $NO_x$, Environ. Sci.
656 Technol., 52, 13738-13746, 10.1021/acs.est.8b03861, 2018.
657 Rosseler, O., Sleiman, M., Nahuel Montesinos, V., Shavorskiy, A., Keller, V., Keller,
658 N., Litter, M. I., Bluhm, H., Salmeron, M., and Destaillats, H.: Chemistry of $NO_x$ on
659 $TiO_2$ Surfaces Studied by Ambient Pressure XPS: Products, Effect of UV Irradiation,
660 Water, and Coadsorbed $K^+$, J.Phys. Chem. Lett., 4, 536-541, 10.1021/jz302119g,
661 2013.
662 Schuttlefield, J., Rubasinghege, G., El-Maazawi, M., Bone, J., and Grassian, V. H.:
663 Photochemistry of adsorbed nitrate, J. Am. Chem. Soc., 130, 12210-+,
664 10.1021/ja802342m, 2008.
665 Schutze, M. and Herrmann, H.: Uptake of the $NO_3$ radical on aqueous surfaces, J.
666 Atmos. Chem., 52, 1-18, 10.1007/s10874-005-6153-8, 2005.
667 Schwartz-Narbonne, H., Jones, S. H., and Donaldson, D. J.: Indoor Lighting Releases
668 Gas Phase Nitrogen Oxides from Indoor Painted Surfaces, Environ. Sci. Technol.
669 Lett., 6, 92-97, 10.1021/acs.estlett.8b00685, 2019.
670 Seltzer, K. M., Vizuete, W., and Henderson, B. H.: Evaluation of updated nitric acid
671 chemistry on ozone precursors and radiative effects, Atmos. Chem. Phys., 15,
672 5973-5986, 10.5194/acp-15-5973-2015, 2015.
673 Shang, J., Xu, W. W., Ye, C. X., George, C., and Zhu, T.: Synergistic effect of
674 nitrate-doped $TiO_2$ aerosols on the fast photochemical oxidation of formaldehyde, Sci.
675 Rep., 7, 10.1038/s41598-017-01396-x, 2017.
676 Shi, Q., Tao, Y., Krechmer, J. E., Heald, C. L., and Ye, Q.: Laboratory Investigation of
677 Renoxification from the Photolysis of Inorganic Particulate Nitrate, Environ. Sci.
678 Technol., 55, 2021a.
679 Shi, Q., Tao, Y., Krechmer, J. E., Heald, C. L., Murphy, J. G., Kroll, J. H., and Ye, Q.:
680 Laboratory Investigation of Renoxification from the Photolysis of Inorganic
681 Particulate Nitrate, Environ. Sci. Technol. 55, 854-861, 10.1021/acs.est.0c06049,

https://doi.org/10.5194/acp-2022-6
Preprint. Discussion started: 27 January 2022


Atmospheric Chemistry and Physics Discussions

682 2021b.
683 Stemmler, K., Ammann, M., Donders, C., Kleffmann, J., and George, C.:
684 Photosensitized reduction of nitrogen dioxide on humic acid as a source of nitrous
685 acid, Nature, 440, 195-198, 10.1038/nature04603, 2006.
686 Sun, Y. L., Zhuang, G. S., Wang, Y., Zhao, X. J., Li, J., Wang, Z. F., and An, Z. S.:
687 Chemical composition of dust storms in Beijing and implications for the mixing of
688 mineral aerosol with pollution aerosol on the pathway, J. Geophys. Res-Atmos., 110,
689 10.1029/2005jd006054, 2005.
690 Tang, M., Liu, Y., He, J., Wang, Z., Wu, Z., and Ji, D.: In situ continuous hourly
691 observations of wintertime nitrate, sulfate and ammonium in a megacity in the North
692 China plain from 2014 to 2019: Temporal variation, chemical formation and regional
693 transport, Chemosphere, 262, 10.1016/j.chemosphere.2020.127745, 2021.
694 Tian, S. S., Liu, Y. Y., Wang, J., Wang, J., Hou, L. J., Lv, B., Wang, X. H., Zhao, X. Y.,
695 Yang, W., Geng, C. M., Han, B., and Bai, Z. P.: Chemical Compositions and Source
696 Analysis of $PM_{2.5}$ during Autumn and Winter in a Heavily Polluted City in China,
697 Atmosphere, 11, 19, 10.3390/atmos11040336, 2020.
698 Verbruggen, S. W.: $TiO_2$ photocatalysis for the degradation of pollutants in gas phase:
699 From morphological design to plasmonic enhancement, J. Photoch. Photobio.C, 24,
700 64-82, 10.1016/j.jphotochemrev.2015.07.001, 2015.
701 Wang, H., Miao, Q., Shen, L., Yang, Q., Wu, Y., Wei, H., Yin, Y., Zhao, T., Zhu, B.,
702 and Lu, W.: Characterization of the aerosol chemical composition during the
703 COVID-19 lockdown period in Suzhou in the Yangtze River Delta, China, J. Environ.
704 Sci., 102, 110-122, 10.1016/j.jes.2020.09.019, 2021.
705 Wang, Z., Ma, Y., Zheng, J., Li, S., Wang, L., and Zhang, Y.: Source apportionment of
706 aerosols in urban Nanjing based on particle size distribution, Huanjing
707 Huaxue-Environmental Chemistry, 34, 1619-1626,
708 10.7524/j.issn.0254-6108.2015.09.2015020303, 2015.
709 Wayne, R. P., Barnes, I., Biggs, P., Burrows, J. P., Canosamas, C. E., Hjorth, J., Lebras,
710 G., Moortgat, G. K., Perner, D., Poulet, G., Restelli, G., and Sidebottom, H.: The
711 nitrate radical-physics, chemistry, and the atmosphere. Atmos. Environ. Part A, 25,

https://doi.org/10.5194/acp-2022-6
Preprint. Discussion started: 27 January 2022


Atmospheric Chemistry and Physics Discussions

712 1-203, 10.1016/0960-1686(91)90192-a, 1991.
713 Ye, C., Gao, H., Zhang, N., and Zhou, X.: Photolysis of Nitric Acid and Nitrate on
714 Natural and Artificial Surfaces, Environ. Sci. Technol., 50, 3530-3536,
715 10.1021/acs.est.5b05032, 2016a.
716 Ye, C., Zhang, N., Gao, H., and Zhou, X.: Photolysis of Particulate Nitrate as a Source
717 of HONO and $NO_x$, Environ. Sci. Technol., 51, 6849-6856, 10.1021/acs.est.7b00387,
718 2017.
719 Ye, C., Zhou, X., Pu, D., Stutz, J., Festa, J., Spolaor, M., Tsai, C., Cantrell, C.,
720 Mauldin, R. L., III, Campos, T., Weinheimer, A., Hornbrook, R. S., Apel, E. C.,
721 Guenther, A., Kaser, L., Yuan, B., Karl, T., Haggerty, J., Hall, S., Ullmann, K., Smith,
722 J. N., Ortega, J., and Knote, C.: Rapid cycling of reactive nitrogen in the marine
723 boundary layer, Nature, 532, 489-491, 10.1038/nature17195, 2016b.
724 Zhou, J. B., Xing, Z. Y., Deng, J. J., and Du, K.: Characterizing and sourcing ambient
725 $PM_{2.5}$ over key emission regions in China I: Water-soluble ions and carbonaceous
726 fractions, Atmos. Environ., 135, 20-30, 10.1016/j.atmosenv.2016.03.054, 2016.
727 Zhou, X. L., Gao, H. L., He, Y., Huang, G., Bertman, S. B., Civerolo, K., and Schwab,
728 J.: Nitric acid photolysis on surfaces in low-$NO_x$ environments: Significant
729 atmospheric implications, Geophy. Res. Lett., 30, 10.1029/2003gl018620, 2003.
730